

Please cite the Published Version

Augusto, KKDL, Gomes-Junior, PC, Longatto, GP, Piccin, E, Cavalheiro, ÉTG, Bernalte, E, Banks, CE  and Fatibello-Filho, O (2025) Electrochemical sensor based on carbon nanohorns and hydrophobic deep eutectic solvent for the determination of serotonin in biological samples. *Electrochimica Acta*, 520. 145836 ISSN 0013-4686

DOI: <https://doi.org/10.1016/j.electacta.2025.145836>

Publisher: Elsevier BV

Version: Accepted Version

Downloaded from: <https://e-space.mmu.ac.uk/638623/>

Usage rights:  [Creative Commons: Attribution 4.0](https://creativecommons.org/licenses/by/4.0/)

Additional Information: This is an author-produced version of the published paper. Uploaded in accordance with the University's Research Publications Policy.

Data Access Statement: Data will be made available on request.

Enquiries:

If you have questions about this document, contact openresearch@mmu.ac.uk. Please include the URL of the record in e-space. If you believe that your, or a third party's rights have been compromised through this document please see our Take Down policy (available from <https://www.mmu.ac.uk/library/using-the-library/policies-and-guidelines>)

Electrochemical sensor based on carbon nanohorns and hydrophobic deep eutectic solvent for the determination of serotonin in biological samples

Karen Kenlder de Lima Augusto^a, Paulo Cardoso Gomes-Junior^a, Gustavo Patelli Longatto^a,
Evandro Piccin^a, Éder Tadeu Gomes Cavalheiro^b, Elena Bernalte^c, Craig E. Banks^c,
Orlando Fatibello-Filho^{a,*}

^a Departamento de Química, Universidade Federal de São Carlos, São Carlos, SP, Brazil

^b Instituto de Química de São Carlos, Universidade de São Paulo, São Carlos, SP, Brazil

^c Faculty of Science and Engineering, Manchester Metropolitan University, Dalton Building, Chester Street, Manchester M1 5GD, Great Britain, UK

Keywords:

Hydrophobic deep eutectic solvent
Carbon nanohorns
Serotonin
Voltammetry
Modified glassy carbon electrode
Biological fluids

A B S T R A C T

A new electrochemical sensor was developed using a hydrophobic deep eutectic solvent (HDES) and carbon nanohorns (CNH) to modify a glassy carbon electrode (GCE). The HDES was based on decanoic acid (DecA) and tetrabutylammonium bromide (TBAB). The performance of the sensor was characterized and optimized using cyclic voltammetry (CV) and electrochemical impedance spectroscopy (EIS), which allowed to determine the ideal amount of HDES in the electrode. Scanning electron microscopy (SEM) and atomic force microscopy (AFM) were used to physically characterize the modified film on the GCE surface. The analytical performance for serotonin (5-HT) determination on the modified electrode (DecA:TBAB(5mg)-CNH/GCE) was evaluated using optimized square-wave voltammetry (SWV). The addition of HDES resulted in a more uniform surface, enabling enhanced electron transfer at the electrode interface and improving the performance for 5-HT detection. The sensor exhibited high sensitivity ($0.20 \mu\text{A L}^{-1} \mu\text{mol}^{-1}$) in the concentration range from 0.50 to $32.71 \mu\text{mol L}^{-1}$ and a low limit of detection (LOD) ($0.09 \mu\text{mol L}^{-1}$) for 5-HT. Additionally, the sensor demonstrated excellent selectivity for detecting 5-HT in the presence of common interferents (concomitants) and displayed good repeatability, reproducibility, and stability. Finally, the sensor was successfully utilized for determining 5-HT in biological fluids, yielding good recovery results.

1. Introduction

Deep eutectic solvents (DES) have sparked significant interest in the field of chemistry due to their well-known characteristics, such as biodegradability, simple preparation process, low toxicity, excellent stability at high temperatures, extraction capacity, and electrochemical characteristics [1]. In addition to this, as a class of environmentally friendly solvents, a comparative study revealed that the EcoScale scores for the DES synthesized, for example, by the heating and stirring were 97, while those for microwave synthesis were 94. According to the authors, scores above 75 indicate an excellent green procedure based on the EcoScale criteria, reinforcing the greener characteristic of these solvents [2]. Moreover, in a study by Simone et al. (2024) [3], focusing on a 3-hour synthesis, the DES used in the work demonstrated successful reusability over four consecutive cycles, achieving a low E-factor of

13.48 and an EcoScale score of 84.5.

In the context of electrochemistry, the use of DES has greatly increased due to their conductive properties, wide potential ranges, and ability to dissolve metal ions. These characteristics make them well-suited for a wide range of electrochemical uses, such as electrodeposition, electropolishing, electroanalysis, and metal extraction and refining [4,5]. Studies have demonstrated the ability of DES to synthesize nanoparticles and electropolymerize conductive polymers, being effective in stabilizing nanomaterials formed in solutions when compared to conventional aqueous mediums. These materials prepared in eutectic medium have been used to modify electrodes for sensing applications [5–8]. Gomes-Junior et al. [9,10], for example, utilized DES to synthesize metallic nanoparticles, which were used to modify the surface of GCE and for applications in food and biological fluids analyses. Particularly, ultrasmall platinum nanoparticles with an average size of 0.208

* Correspondent author.

E-mail address: bello@ufscar.br (O. Fatibello-Filho).

nm were synthesized using a DES based on choline chloride and urea, owing to its exceptional stabilization properties. Moreover, Buoro et al. [11] used ternary deep eutectic solvents for the electrodeposition of poly (cresyl violet) on multiwalled carbon nanotube-modified glassy carbon electrodes. The modified sensor was then used for the determination of hydroquinone in dermatological creams.

Moreover, regarding biological compounds, the literature reports the use of DES to develop new electrochemical sensors that can enhance the detection of important substances such as biomarkers and neurotransmitters, as these compounds play a crucial role in diagnostic applications [10,12–15]. Prathish et al. [12], for example, explored the electropolymerisation of poly(3,4-ethylenedioxythiophene) (PEDOT) films on glassy carbon electrodes, using DES as the polymerisation medium. The study revealed that the DES played a crucial role in the morphology, size, surface characteristics, electrocatalytic activity, and overall sensing properties of the PEDOT films. The modified electrodes exhibited excellent performance in the simultaneous detection of biomarkers. Moreover, in a 2024 study by Uysal et al. [14], the authors developed a novel electrochemical sensor for detecting epinephrine by electropolymerizing toluidine blue onto glassy carbon electrodes modified with Fe₃O₄ nanoparticles on DES medium. The incorporation of Fe₃O₄ nanoparticles and DES significantly enhanced the sensor's electrocatalytic activity, leading to improved sensitivity and selectivity in epinephrine detection.

In particular, serotonin (5-HT), as a vital neurotransmitter, plays an important role in the human body by regulating emotions, mood, appetite, and sleep. Monitoring 5-HT levels in the body is crucial as abnormal concentrations can be linked to various diseases and disorders [16]. Normal 5-HT levels typically range from 270 nM to 1490 nM in serum samples and from 300 nM to 1650 nM in urine [17]. Therefore, it is important to invest in sensitive methods capable of detecting 5-HT in a simple and rapid manner. Electrochemical techniques are promising in these aspects owing to their low cost and ease of operation, short analysis times and production of results characterised by high precision and sensitivity [17,18].

The literature presents various electrochemical sensors modified with different materials, such as metallic nanoparticles, conductive polymers, and carbon materials for the 5-HT determination [19–23]. Tertis et al. (2017) [19], for example, developed an electrochemical sensor featuring a three-dimensional structure made with polypyrrole nanoparticles integrated with gold nanoparticles. The polypyrrole enhanced the active surface area, while the gold nanoparticles contributed to the catalytic properties of the sensor, which improved the 5-HT detection. The sensor showed an analytical performance 320 times superior to the bare electrode, with a limit of detection of ~33 nM, emphasising the benefits of this customized hybrid surface. On the other hand, utilizing atomic layer deposition, Ran et al. (2021) [20] constructed a sensor using a nanocomposite based on Ni nanoparticles-reduced graphene oxide. This sensor showed a broad linear detection range from 0.02 to 2 μM with a detection limit of 0.01

μM. The authors presented its remarkable electrocatalytic activity towards 5-HT detection. Although these works have shown excellent electrochemical performance towards 5-HT determination, some of them involve complex synthesis processes or the use of expensive materials for sensor development. For example, in a work reported by Babulal et al. (2023) [21], the authors developed an electrochemical sensor for serotonin detection with excellent performance, catalytic activity, anti-fouling properties, high selectivity, and reproducibility. However, the electrode modification process was labour-intensive. In another example, Koluçak et al. (2018) employed a pre-treatment process for multi-walled carbon nanotubes involving boiling the carbonaceous material in concentrated nitric acid [22].

To enhance the sensitivity, conductivity, and analytical response of electrodes, it is convenient to use simpler materials that can be easily prepared for the electrode modification process. Ideally, this process should avoid the use of excessive toxic chemicals or harsh conditions,

ensuring both efficiency and sustainability. In view of this, DES is an interesting choice based on their electrochemical properties. Many researchers investigated the role of these solvents in the preparation of electrodes for different target analytes [9–11,24–26]. However, while most studies focus on using DES as a medium to prepare materials for electrode modification, few have employed DES directly in the modification process itself. Nevertheless, there are notable studies that have successfully utilised DES for electrode modification. In previous studies [26], it was demonstrated that using a deep eutectic solvent composed of choline chloride and glycerol together with carbon black and a cross-linked chitosan film improved the kinetic parameters of the glassy carbon electrode. On the other hand, Augusto et al. (2022) [24] investigated the use of various hydrophobic deep eutectic solvents to modify carbon paste electrodes for hydroquinone determination. The study showed that incorporating HDES into the carbon paste significantly improved the electroanalytical properties of the electrode. Other studies of using DES in the development of carbon paste electrodes revealed lower charge transfer resistance for electrodes modified with natural deep eutectic solvents, which yielded higher peak currents for the oxidation-reduction of dopamine and ascorbic acid [25]. Moreover, the use of a DES based on choline chloride and 4-methoxybenzyl alcohol in combination with SWCNT-ZrO₂ to form a CPE/DES/SWCNT-ZrO₂ electrochemical sensor showed excellent catalytic activity for the simultaneous determination of paracetamol and rizatriptan [27].

Regarding serotonin detection, only few works have investigated the performance of electrodes modified with DES [28,29]. For example, Atici et al. (2023) [28] constructed a modified electrode by integrating zinc oxide nanorods (ZnONR), polymethylene blue (PMB), which was prepared in 90 % DES ethaline solution and 10 % 50 mM pH 8.0 phosphate buffer, and gold nanoparticles (AuNPs) on screen-printed carbon electrodes (SPCEs). The synergistic effects of ZnONRs, PMB, and AuNPs enhanced the sensor's electrochemical properties, such as electron transfer rate and conductivity, making it highly effective for serotonin detection. Also, Kabaca et al. (2023) [29], utilised a deep eutectic solvent based on ethylene glycol and choline chloride to electropolymerise Nile blue on the surface of SPCE/TiO₂NP/AuNP electrode. The resulting SPCE/TiO₂NP/AuNP/PNB_{DES} sensor was used for the simultaneous determination of dopamine and serotonin in blood serum. Again, DES served only as a medium for preparing a polymer and not as a modification agent as performed in this proposed work.

This paper provides a detailed investigation of the effects of HDES as a modifier on the electrode surface. The electrochemical sensors were constructed using a suspension of carbon nanohorns in HDES (prepared from decanoic acid and tetrabutylammonium bromide), which was applied on the surface of glassy carbon electrodes. We aimed to find the optimal amount of HDES in the suspension to achieve enhanced electrochemical performance towards serotonin detection. This study was performed by electrochemical impedance spectroscopy and cyclic voltammetry. The morphology and topography of the composite film were also characterized. Finally, the modified electrode was used to quantify serotonin in synthetic biological fluids.

2. Experimental

2.1. Chemicals

All chemicals were of analytical grade and used as received without any further purification. All solutions were prepared with ultrapure water (resistivity ≥ 18.0 MΩ cm) obtained from a Millipore Milli-Q system (Billerica, USA). Tetrabutylammonium bromide (≥ 99.0 %), serotonin hydrochloride (≤ 100 %), bovine calf serum (sterile-filtered, hemoglobin ≤ 35 mg/dL), and carbon nanohorns were purchased from Sigma-Aldrich (St. Louis, USA). Decanoic acid (≥ 98.0 %) was acquired from Neon (São Paulo, Brazil). Potassium phosphate monobasic (≥ 99 %) and potassium phosphate dibasic (≥ 99 %) were acquired from Synth (Diadema, São Paulo). A phosphate buffer solution (PB) of 0.20 mol L⁻¹

pH 7.0 was used as a supporting electrolyte. A 1.0×10^{-2} mol L⁻¹ 5-HT standard stock solution was prepared by dissolution in PB solution. Dilution processes were adopted to obtain different concentrations of standard solutions.

2.2. Apparatus

DSC curves were obtained in a Q10 Differential Scanning Calorimetric module, controlled by the Thermal Advantage Series® software (v.5.5.24), while sub ambient temperatures were reached with the help of a RCS cooling accessory, all from TA Instruments (New Castle, USA). Analyses were carried out using sample mass of (5.0 ± 0.1) mg, at a heating rate of 10 °C min⁻¹, under a dynamic N₂ atmosphere flowing at 50 mL min⁻¹. Closed aluminium sample holders with a pin hole in the centre of the lid ($\phi = 0.7$ mm) were used in all experiments. The measurements were performed in the temperature range of 223.15 – 393.15 K. The endothermic peak temperatures were used to characterize the melting event.

Morphological characterization of the composite films was carried out on a field-emission gun scanning electron microscopy (FEG/SEM, FEI Magellan 400 L). Also, an atomic force microscopy (Bruker Nanoscope 6 Multimode 8) was used to acquire the film topography and for roughness characterization.

Electrochemical measurements were conducted using an Autolab (Metrohm) potentiostat/galvanostat model PGSTAT101, and data was collected using NOVA 2.1.6 software. EIS measurements were performed in the frequency range of 0.1 Hz to 65 kHz, applying a potential of 0.35 V and 0.010 V of signal amplitude to perturb the system on a Sensi Smart potentiostat (PalmSens, The Netherlands) using the PStrace 5.9 software for data acquisition. A conventional three-electrode system was used, with a platinum plate as a counter electrode (area 1.0 cm²), the reference electrode used was Ag/AgCl/KCl (3.0 mol L⁻¹), and a GCE (with or without modification) as the working electrode ($d = 3.0$ mm). The catalytic rate constant (k_{cat}) of 5-HT oxidation in the proposed film was carried out using chronoamperometry, applying a potential of 0.35 V and an interval time of 0.01 s.

2.3. Preparation of hydrophobic deep eutectic solvent

The hydrophobic deep eutectic solvent used in this work was based on decanoic acid and tetrabutylammonium bromide in a molar ratio of 2:1 (DecA:TBAB), as previously reported by Augusto et al. (2022) [24]. The synthesis was conducted in a closed glass vessel at a temperature of 353.15 K and stirring at 500 rpm for approximately 1 h (heating plate, RH basic 1, IKA), resulting in a uniform liquid. The melting point of the HDES was assessed through DSC.

2.4. Preparation of glassy carbon electrodes modified with DecA:TBAB

Herein, we modified the GCE using a suspension containing DecA:TBAB and CNH. The effect of DecA:TBAB amount (0, 3, 5, 8, and 10 mg) in the suspension was carefully studied by CV and EIS. Prior to the modification, the GCE surface was polished with 0.5 µm alumina slurry and washed with deionized water. The modifying dispersions containing DecA:TBAB and CNH were prepared as follows: 1.0 mg of CNH was suspended in 980 µL of N,N-dimethylformamide (DMF) with 20 µL of Nafion™, and DecA:TBAB. The suspensions were sonicated for 30 min in an ultrasonic bath for complete dispersion of the materials. Then, 10.0 µL of these suspensions were dropped on the GCE surface and allowed to dry in a desiccator for roughly 2 h until the film was formed.

2.5. Synthetic urine and bovine serum preparation

Synthetic urine samples were prepared using the method previously described by Laube et al. [30], with 0.20 mmol L⁻¹ KCl, 0.18 mmol L⁻¹ NH₄Cl, 0.10 mmol L⁻¹ NaCl, 0.10 mmol L⁻¹ CaCl₂, 0.15 mmol L⁻¹

KH₂PO₄, and 0.18 mmol L⁻¹ urea in a 25 mL volumetric flask. This sample was spiked with three concentrations of 5-HT (2.0, 3.0 and 5.0 µmol L⁻¹, respectively) and recovery percentages were calculated accordingly. Similarly, the serum (bovine serum) sample was diluted 10 times with ultrapure water, spiked with three known concentrations of 5-HT (2.0, 3.0, and 5.0 µmol L⁻¹, respectively), and analysed by calculating the recovery percentage.

3. Results and discussion

3.1. HDES: green synthesis

To better assess the environmental sustainability of the HDES synthesis, we quantified its greenness by calculating the Environmental Factor (E-factor) [31], the electrical energy consumption during the synthesis [2], and the EcoScale [32] for producing approximately 10 mL of HDES over a 1-hour process.

The E-factor is a metric used to evaluate the environmental impact of a chemical process. It is calculated as the ratio of the total waste mass-generated to the desired product's mass [31]. For DES, the E-factor calculation is generally straightforward because these solvents are typically synthesized through simple mixing without producing significant byproducts. As a result, waste is often negligible, with the components almost entirely incorporated into the final product (100 % atomic efficiency) [33].

In this work, the HDES synthesised was based on 1 mol of DecA (172.26 g) and 0.5 mol of TBAB (161.18 g), yielding 333.44 g of HDES (100 % atomic efficiency), *i.e.* the components were fully incorporated into the product, resulting in an E-factor of 0, reflecting a waste-free process. The E-factor may increase slightly during synthesis in cases of minor losses, such as spillage or non-recoverable residues. Nevertheless, it remains low, highlighting that the DES synthesis has an environmentally friendly nature.

Furthermore, the electric energy consumption for the synthesis of HDES was assessed through Eq. (1) [2].

$$\text{Consumption} = \frac{P \cdot t / 1000}{V} \quad (1)$$

In this context, consumption (kWh) represents the electrical energy used during synthesis, P is the equipment power (W), t (h) is the time of synthesis, and V (mL) corresponds to the volume of HDES prepared. The electric energy consumption calculated for the HDES was 0.0415 kWh mL⁻¹, with an EcoScale score of 90. In fact, the HDES synthesis involves simple mixing of components with low energy consumption, without byproducts as discussed and yields of approximately 100 %. All these values are in accordance with previous works in the literature for DES synthesis and application in different processes [2,3].

3.2. HDES melting point

Melting temperature of the DecA:TBAB HDES was measured using DSC. Fig. 1 shows the DSC curves for TBAB, DecA, and 2:1 (mol/mol) DecA:TBAB mixture with the temperatures of all thermic events.

In Fig. 1a, the curve for TBAB is displayed, where two endothermic peaks are presented. The first peak at 362.8 K could be attributed to crystal readjustment and conformational disorder [34]. In contrast, the second peak at 376.2 K is relative to its melting point, in agreement with the melting temperature of the pure compound declared by the supplier. The decanoic acid (Fig. 1b) showed a sharp melting peak at 305.5 K, which agrees with the reported melting temperature of the pure compound [35].

The DSC curve for the HDES (Fig. 1c) revealed a melting temperature below 273.15 K. The thermal behaviour for the DecA:TBAB system presented four thermal events. Two are related to the characteristic transitions of the phase transformation of fatty acids (252.7/endo and 260.3 K/exothermic) [36]. A third endothermic peak occurred from the

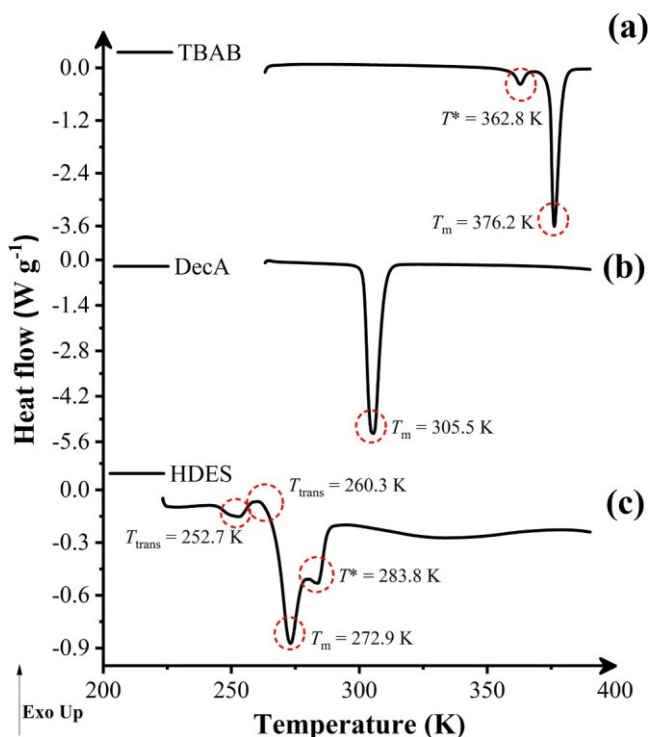


Fig. 1. DSC curves with the thermal events of the pure components (a) TBAB and (b) DecA and for the (c) HDES (DecA:TBAB). Heating rate: $10\text{ }^{\circ}\text{C min}^{-1}$ under a dynamic N_2 flow of 50 mL min^{-1} ; measurements were taken from 223.15 to 393.15 K, with endothermic peak temperatures used to characterize the melting event.

free fraction of DecA at 283.8 K. Lastly, an endothermic peak at 272.9 K was attributed to the melting temperature of the DecA:TBAB system.

It is worth noting that the first peak of the DSC curve, nearly 225 K for DecA:TBAB, is related to the thermal inertia effect, which could be attributed to a gradient of temperature created between the end of the cooling process and the beginning of the heating of the sample [36], associated with the experiment process, in which an isotherm was applied for 5 min during the cooling process prior the heating of the sample.

3.3. Effect of modifying the GCE with HDES: an electrochemical study towards the 5-HT analytical response

In our first study, we evaluated the impact of adding increasing amounts of HDES within the suspension with CNH on the GCE surface. The investigation sought to examine the effectiveness of this approach in enhancing the performance of the GCE. Different amounts of DecA:TBAB were studied: 0, 3, 5, 8, and 10 mg. The study was conducted using CV and EIS, and $100\text{ }\mu\text{mol L}^{-1}$ 5-HT in 0.2 mol L^{-1} PB pH 7.0. Fig. 2a shows the CV results for all electrodes.

It can be observed that the analytical signal improved as the DecA:TBAB content in the film increased up to a concentration of 5 mg. From 8 mg of DecA:TBAB, the oxidation peak for 5-HT slightly decreased. This phenomenon is more apparent when evaluating the peak currents and potentials shown in Fig. 2c and d. The GCE electrode did not exhibit a well-defined oxidation peak to 5-HT, as demonstrated in Fig. 2. Compared to the CNH/GCE electrode (which had 0 mg of DecA:TBAB), the 5 mg electrode improved the analytical current by 5-fold (Fig. 2b). Furthermore, even the electrodes with concentrations of 3 and 10 mg enhanced the peak current by approximately 3-fold despite presenting lower peak currents among the electrodes modified with HDES.

It is important to note that all concentrations of DecA:TBAB caused a shift in the peak potential towards more negative values. This suggests

that modifying the electrode with HDES may have a catalytic effect. The electrodes with 3 and 5 mg of HDES showed a decrease of 36 mV compared to CNH/GCE and an increase of current of $8\text{ }\mu\text{A}$ for the 5 mg HDES modified electrode.

Furthermore, as shown in the EIS results, Fig. 3a and Table 1 the presence of 5 mg HDES decreased the resistance of charger transfer (R_{ct}) in 127 and 2-folds compared with GCE and CNH/GCE, respectively. Also, the higher value of the R_{ct} ($34.75\text{ k}\Omega$) for GCE explains why it was not possible to observe a defined oxidation peak for the 5-HT at this electrode, indicating that the bare electrode is not suitable for 5-HT determination. By modifying the electrode with CNH, the reactions that occur in the interface between the electrode and the solution have been improved. The 5-mg electrode has shown better results compared to GCE and CNH/GCE, with a significant improvement in the apparent heterogeneous electron-transfer rate constant (k_{app}) by 255 and 1.7-folds, respectively. Furthermore, it performed better compared to all the electrodes in this study.

The improvement achieved by modifying the electrodes with HDES may be due to the conductivity provided by the solvent ($51.5\text{ }\mu\text{S cm}^{-1}$, as previously stated by Augusto et al. [24]), which, in turn, enhances the overall conductivity of the electrode. Additionally, as discussed further, the HDES could lead to a more uniform suspension by coating the CNH particles. This could be observed by the α value, which was 0.81 for the electrode modified with 5 mg of DecA:TBAB. This value was close to the GCE value of 0.85. The α represents the roughness associated with capacitance measurements in the EIS, where $\alpha = 1$ represents a smooth surface [37]. As mentioned in Section 3.3, it was observed that the surface of the CNH/GCE electrode is irregular. The α value obtained for this electrode is consistent with this observation. It is possible that such unevenness may have also occurred in the other electrodes that were modified with different amounts of HDES. This is evident as these electrodes exhibit a similar α value to the CNH/GCE electrode. Additionally, the decrease in the analytical signal could be attributed to the higher viscosity of the HDES ($597\pm 10\text{ mPa s}$ [24]). The viscosity of the HDES affects the conductivity of the film, and it could possibly lower the redox reactions at the electrode surface.

Additionally, using EIS allows for the impedance magnitude to be used as a comparison parameter, which results from the resistive and capacitive behaviours of the electrode at a specific frequency [38]. The Bode plot in Fig. 3b shows a graph of impedance magnitude ($|Z|$) versus frequency for all modified electrodes. As expected, at low frequencies (between 10^{-1} and 10^1 Hz), the graph displays a linear decrease in the response of $|Z|$. However, as the frequency increases, the $|Z|$ reaches a plateau. This pattern can be observed from around 10^2 Hz to higher frequencies [38]. In general, all the modified electrodes demonstrated lower impedance values compared to the GCE and CNH/GCE electrodes, indicating that the resistance of the material has decreased, leading to an improved flow of electrons through the electrode film. This can be attributed to the inclusion of HDES, as the deep eutectic solvent contributed to improving the electrical conductivity [24,39]. Hence, the electrode modified with 5 mg of HDES was chosen for further experiments.

Additionally, a study related to the storage of faradaic charge generated by the redox reaction of 5-HT on the sensor surface was carried out by determining the specific faradaic capacitance, C_s . Carbonaceous materials can accumulate charges originated from the diffusional mass transport of the redox reaction of the electroactive species on their surface [40]. Therefore, C_s of the CNH/GCE and DecA:TBAB(5mg)-CNH/GCE sensors through the 5-HT electrooxidation process was determined by CV to attest the enhancements in faradaic charge storage properties that may result from the diffusion process of the target analyte (see Section 3.6), using Eq. (2), which results from the proposed model for the CV analysis [41]

$$C_s = \frac{A}{2\Delta V m \nu} \quad (2)$$

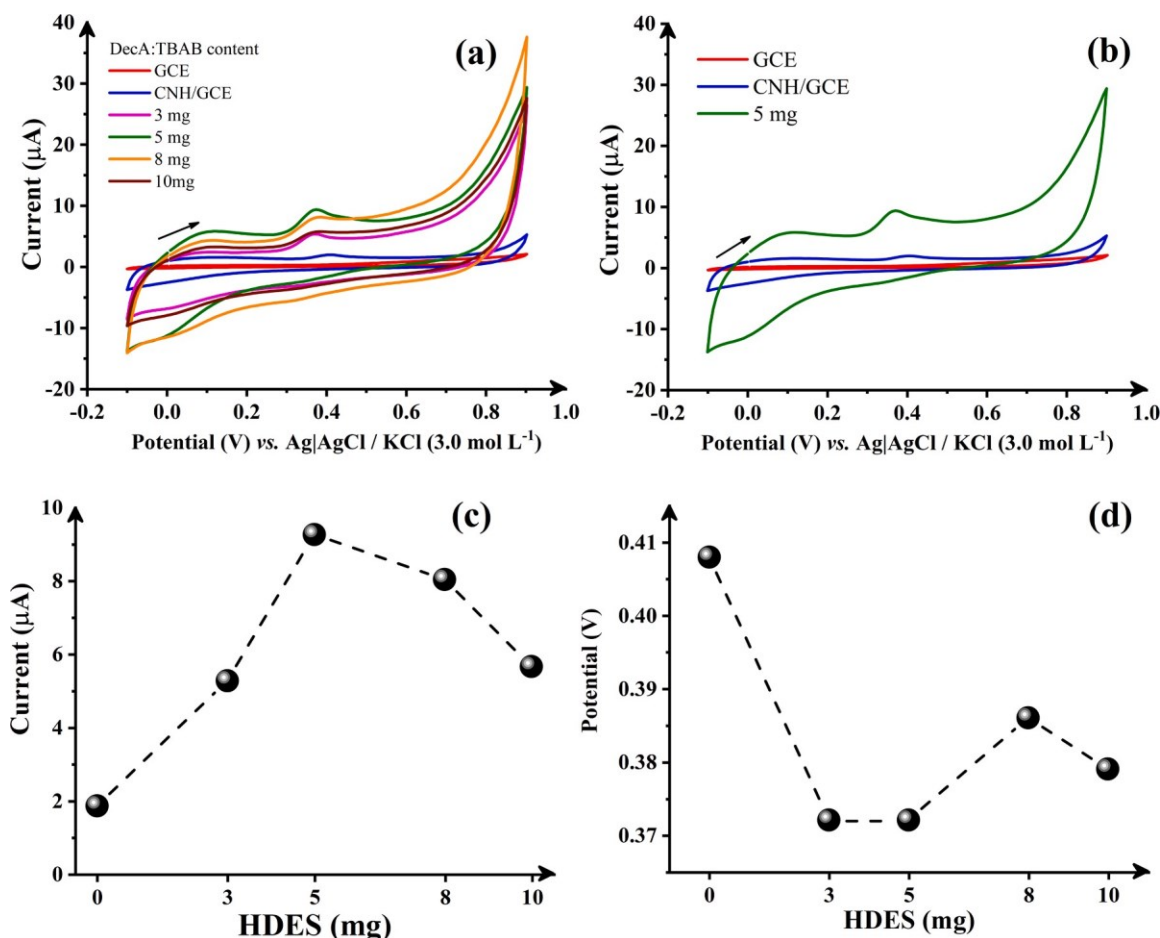


Fig. 2. CV results (a) and (b) obtained for the oxidation of $100 \mu\text{mol L}^{-1}$ 5-HT in 0.2 mol L^{-1} PB pH 7.0 using (—) GCE and electrodes with different amounts of DecA:TBAB HDES: (—) CNH/GCE (0 mg), (—) 3 mg, (—) 5 mg, (—) 8 mg, and (—) 10 mg. Scan rate: 50 mV s^{-1} . Plots of (c) I_{ap} and (d) E_{ap} versus the amount of HDES.

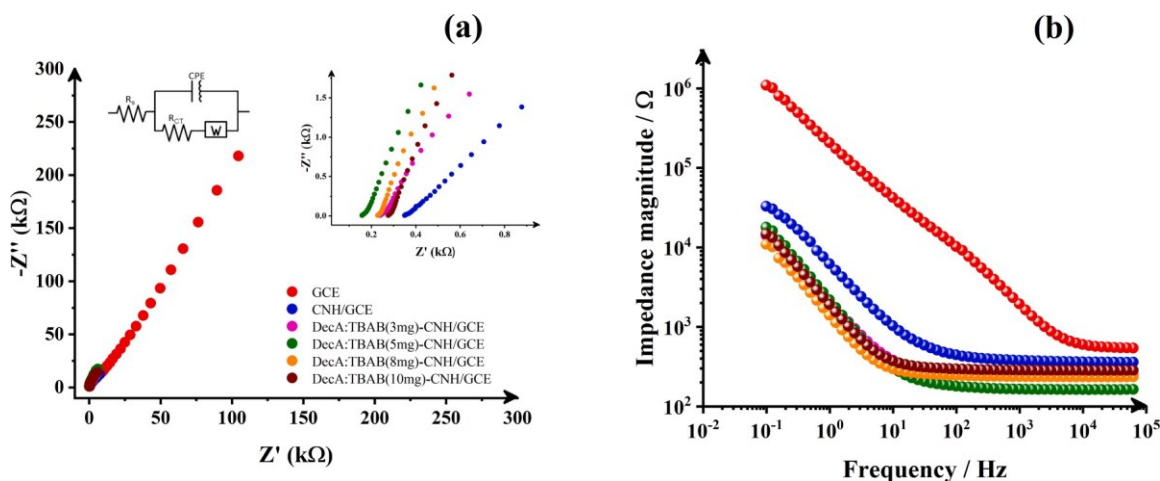


Fig. 3. Nyquist plots (65,000–0.1 Hz) (a) using $100 \mu\text{mol L}^{-1}$ 5-HT in 0.2 mol L^{-1} PB pH 7.0 at (●) GCE, (●) CNH/GCE, (●) DecA:TBAB(3mg)-CNH/GCE, (●) DecA:TBAB(5mg)-CNH/GCE, (●) DecA:TBAB(8mg)-CNH/GCE, (●) DecA:TBAB(10mg)-CNH/GCE. Inset: the proposed equivalent circuit. In (b) The Bode plot of impedance magnitude versus frequency.

where C_s is the specific faradaic capacitance (F g^{-1}), A is the integrated area of the cyclic voltammogram for the 5-HT CVs (A V) (see Figure S1), m is the mass of active material (g), ν is the potential scan rate of CV (V s^{-1}), and ΔV is the potential window of CV (total voltage range). The C_s values were 0.027 and 0.071 F g^{-1} for the CNH/GCE and DecA:TBAB

(5mg)-CNH/GCE, respectively. These values suggest that when the electrode is modified with DES, the faradaic responses to 5-HT increase 2.6-fold compared to CNH/GCE, denoting the material's catalytic enhancement and ability to store charges in the electrooxidation process. Sensor modifications generally increase the faradaic capacitance,

Table 1EIS data for 100 $\mu\text{mol L}^{-1}$ 5-HT in 0.2 mol L^{-1} PB pH 7.0.

Electrode	R_s / Ω	R_{ct} / Ω	α	$k_{app} / \text{cm s}^{-1}$
GCE	498.5	34,753.0	0.85	3.8×10^{-5}
CNH/GCE	349.6	468.5	0.70	5.7×10^{-3}
DecA:TBAB(3mg)-CNH/GCE	238.9	502.6	0.71	5.3×10^{-3}
DecA:TBAB(5mg)-CNH/GCE	158.0	274.1	0.81	9.7×10^{-3}
DecA:TBAB(8mg)-CNH/GCE	228.4	761.1	0.72	3.5×10^{-3}
DecA:TBAB(10mg)-CNH/GCE	276.5	456.5	0.75	5.8×10^{-3}

whether with carbonaceous materials or nanoparticles [42]. In the case

of the modification with HDES, functional groups present in the structures of these solvents are incorporated into the film composition,

making it more efficient in the electrooxidation of serotonin. Although some works in the literature show adsorptive effects for 5-HT [43,44], the HDES-based sensor did not show a pronounced effect, probably due to the hydrophobic nature of the film. As observed in the AFM results, the coating of the film made it more homogeneous, which reduces the adsorptive effects of the target analyte.

3.4. Physical characterization of the electrode

In this study, we used SEM analysis to examine the surface morphology of the CNH. The SEM image in Fig. 4a displays spherical aggregates of the CNH within the proposed film with HDES. This is consistent with previous literature, which has shown that carbon nanohorns can form spherical aggregates known as dahlia, bud, and seed aggregates based on their appearances [45].

Based on the SEM image, it seems that the presence of HDES did not alter the morphology of the carbon material. However, the 3D-topography images obtained using AFM (Fig. 4b and c) suggest that the presence of HDES coated the carbon nanomaterial, resulting in a more uniform surface compared to the rough surface without HDES. These results align with those discussed in Section 3.2, where the electrode with HDES exhibited a higher α value compared to the electrode without HDES (CNH/GCE), indicating a smoother surface. To confirm this, we calculated the root mean square (RMS) roughness (R_q) for both surfaces modified with and without the HDES-containing film. The results showed an R_q value of 34.93 nm for the surface without HDES and a lower value for the film with HDES, 6.32 nm. These findings support the idea that adding HDES to the suspension generated a more uniform and thin film, which facilitates electron transfer in the electrode-solution interface as illustrated in Scheme 1, where the CNH particles are coated with the eutectic solvent.

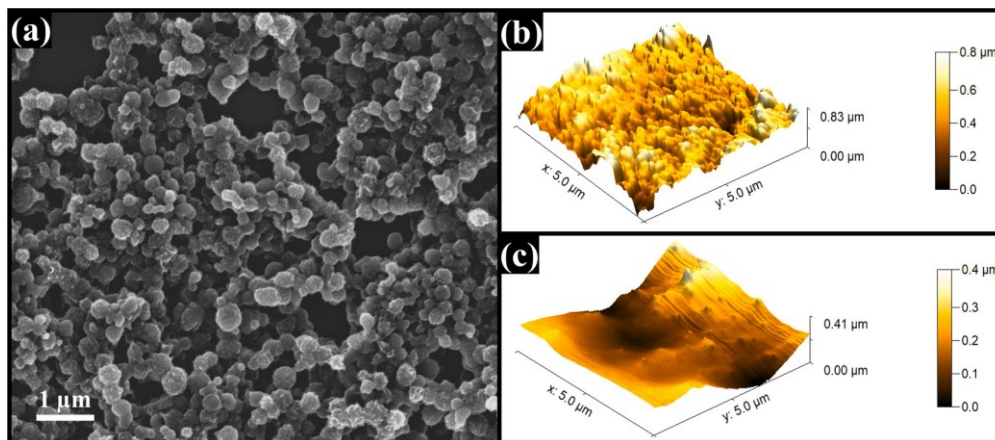


Fig. 4. (a) SEM image of carbon nanohorns at 100,000x magnification. 3D AFM topography images for (b) CNH suspension and (c) DecA:TBAB+CNH suspension.

3.5. Catalytic rate constant for serotonin oxidation and electroactive surface area

The catalytic rate constant (k_{cat}) of the oxidation of serotonin was calculated based on data obtained from a chronoamperometry study using 100 $\mu\text{mol L}^{-1}$ serotonin at a fixed potential of 0.35 V (Figure S2). This study compared the influence of adding HDES in the film to modify the electrode, and it was carried out using the GCE, CNH/GCE, and DecA:TBAB(5mg)-CNH/GCE. The k_{cat} value of 5-HT oxidation was calculated using the slope of the plot of I_{cat}/I_L vs. $t^{1/2}$ (Figure S2 inset) with the Eq. (3) [46]

$$I_{cat}/I_L = \pi^{1/2}(k_{cat} ct)^{1/2} \quad (3)$$

where I_{cat} and I_L are the catalytic and diffusion-limited current (A) responses in the presence and absence of 5-HT, c is the concentration of 5-HT (mol L^{-1}), and t is the time (s). The obtained k_{cat} values were 2.7×10^2 , 4.1×10^3 , and 9.0×10^3 mol $^{-1}$ L s $^{-1}$ for GCE, CNH/GCE, and DecA:TBAB(5mg)-CNH/GCE, respectively. These values showed an increase of 2.4 and 34-fold in the k_{cat} value compared to CNH/GCE and GCE, respectively. The values obtained for the k_{cat} using the CNH/GCE and DecA:TBAB (5mg)-CNH/GCE electrodes presented the same magnitude as a report in the literature for 5-HT [47]. This supports the results observed in EIS and CV regarding the catalytic performance of the proposed modified electrode towards oxidizing serotonin.

Cyclic voltammetry experiments were conducted to assess the electroactive areas of bare GCE, CNH/GCE, and DecA:TBAB(5mg)-CNH/GCE electrodes. A 100 $\mu\text{mol L}^{-1}$ 5-HT solution was prepared in a supporting electrolyte, consisting of 0.2 mol L^{-1} phosphate buffer at pH 7.0, and cycled at potential scan rates from 15 to 100 mV s $^{-1}$ (see Fig S3a, b, and c). The electroactive area was calculated using the modified Randles-S \check{e} v \check{c} ik equation for irreversible systems (Eq. (4)) [48]:

$$I_p = 2.99 \times 10^5 \alpha^{1/2} c D^{1/2} A v^{1/2} \quad (4)$$

Following Eq. (4), I_p is the anodic peak current (A), D is the diffusion coefficient of 5-HT (9.0154×10^{-6} cm 2 s $^{-1}$ [49]), A is the electroactive area (cm 2), c is the concentration of 5-HT (1.0×10^{-7} mol cm 3), v is the potential scan rate (V s $^{-1}$), and α is the transfer coefficient, a measure of symmetry of the energy barrier for a single electron transfer step. For an irreversible reaction, α can be calculated from the relation $|E_p - E_{p/2}| = 47.7/\alpha$ [48]. The electroactive areas for bare GCE, CNH/GCE, and DecA:TBAB(5mg)-CNH/GCE electrodes are 0.012, 0.10, and 0.75 cm 2 , respectively. These results suggest that adding the HDES into the film increased the electroactive area by 62 and 7.5-fold, compared to the



Scheme 1. Suggested electrochemical mechanism for serotonin oxidation at the DecA:TBAB(5mg)-CNH/GCE modified electrode.

bare GCE and CNH/GCE, respectively. The results indicate that, in addition to the synergistic interaction between HDES and CNH, the enhanced electroactive surface area also played a crucial role in facilitating the serotonin oxidation.

3.6. pH and scan rate studies

To study the dependence of serotonin oxidation on the pH, a study was carried out using square-wave voltammetry for $100 \mu\text{mol L}^{-1}$ 5-HT in 0.1 mol L^{-1} Britton-Robinson (BR) buffers in the pH range from 2.0 to 12.0 (Fig. S4a). The results in the inset of Fig. S4a show a linear correlation between the peak potential and pH. As pH increased, the E_{ap} shifted towards more negative values. The slope of E_{ap} vs. pH was 47 mV pH^{-1} , indicating that only one proton was involved in the two-electron oxidation process of 5-HT. This behaviour has also been reported in other studies [23,50]. In addition, the I_{ap} vs pH plot (Fig. S4b) shows that the peak current reaches its maximum at pHs 6.0 and 7.0 and decreases in more basic mediums. Considering this result and the lower standard deviation of the measurements, pH 7.0 was selected for further experiments. Moreover, in a study of supporting electrolytes, a 0.2 mol L^{-1} PB solution at pH 7.0 was compared with BR buffer. Due to improvements in peak current, PB was chosen as the supporting electrolyte.

A potential scan rate effect on the electrode response was performed to determine which process controls the oxidation reaction of serotonin in the interface electrode solution. CV was carried out in $100 \mu\text{mol L}^{-1}$ 5-HT in 0.2 mol L^{-1} PB pH 7.0 at potential scan rate from 15 to 100 mV s^{-1} . Fig. S3 (a, b, and c) shows the voltammograms with the plots for I_{ap} vs. $v^{1/2}$ inset. Table S2 shows the data obtained in the plots for I_{ap} vs. $v^{1/2}$, $\log(I_{\text{ap}})$ vs. $\log(v)$, and I_{ap} vs. v .

The logarithm of current versus the logarithm of the potential scan rate plot can help determine whether a process is diffusion-controlled or adsorption-controlled. A slope closer to 0.5 indicates a diffusion-controlled process, while a value closer to 1 indicates an adsorption-controlled process [51]. In this experiment, the logarithm of I_{ap} and v showed a linear relationship for all the electrodes (Table S2). The slopes for GCE and CNH/GCE were 0.37 and 0.50, respectively. This means that the reaction for 5-HT is diffusion-controlled in both electrodes. On the other hand, the slope of the logarithmic curve for DecA:TBAB (5mg)-CNH/GCE was 0.80. This indicates that the oxidation of serotonin may be controlled by both adsorption and diffusion. However, it can be observed from the data of I_{ap} vs. $v^{1/2}$ plot a linear increase of the peak current with the square root of the scan rate, indicating a predominance of a diffusion process. These findings are consistent with other works in the literature, where the redox reaction of serotonin is also controlled by the diffusion process [20,52].

3.7. Analytical performance

To improve the determination of 5-HT, the SWV parameters were optimized. Table S1 shows the results for the optimization of amplitude (a), frequency (f), and potential increment (ΔE_s) based on the oxidation response of serotonin at the proposed electrode, DecA:TBAB(5mg)-CNH/GCE.

Under optimal conditions, an analytical curve for 5-HT oxidation was constructed in the concentration ranging from 0.50 to $32.71 \mu\text{mol L}^{-1}$. Fig. 5 shows the SW voltammograms obtained using DecA:TBAB (5mg)-CNH/GCE electrode and the corresponding linear plot for this concentration range. The LOD was calculated using the equation: $3 \times \sigma/\text{slope}$, where σ is the standard deviation of 10 measurements of the blank (0.2 mol L^{-1} PB pH 7.0). The LOD was 90 nmol L^{-1} .

The results obtained in this study were compared to those reported in the literature for the electrochemical determination of serotonin. As observed in Table 2, the figures of merit were satisfactory in relation to the other sensors. It is important to highlight that the electrode proposed in this work, which was modified with HDES, showed overall good electroanalytical performance. A significant advantage of this approach compared to other studies in the literature is the simplicity and sustainability of the fabrication process, driven by the greener nature of DES. The eutectic solvent was prepared in a simple manner and used directly to modify the surface of the GCE, without any pre-treatment or additional steps. This method not only reduces the need for complex modification steps but also aligns with environmentally friendly practices, offering a more accessible alternative to other electrodes reported

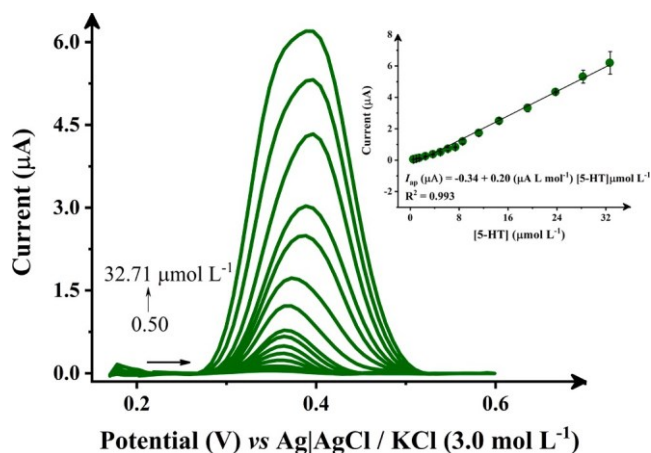


Fig. 5. SW voltammograms for 5-HT oxidation in 0.2 mol L^{-1} PB pH 7.0 in a concentration range of 0.50 to $32.71 \mu\text{mol L}^{-1}$. SWV parameters: a : 10 mV , f : 5 Hz , and ΔE : 8 mV . Inset: the linear plot and equation: $I_{\text{ap}} (\mu\text{A}) = -0.34 + 0.20 (\mu\text{A L mol}^{-1}) [5\text{-HT}] \mu\text{mol L}^{-1}$ ($R^2 = 0.993$).

Table 2

Comparison of the analytical parameters for the voltammetric determination of serotonin.

Electrode	Technique	Sensitivity / $\mu\text{A L}^{-1} \mu\text{mol}^{-1}$	Linear range/ $\mu\text{mol L}^{-1}$	LOD / $\mu\text{mol L}^{-1}$	Ref
Fe ₃ O ₄ -MWCNT-poly (BCG)/GCE	DPV	0.5309	0.5 – 100.0	0.08	[53]
NDs-AuNPs-Gr-CSN/GCE	DPV	0.18	0.3 – 3.0	0.100	[54]
MWCNT-PANI/GCE	DPV	0.7977	0.1 – 12.0	0.033	[22]
AuNPs@PPyNPs-based sensor	SWV	0.3316	0.1 – 15.0	0.03322	[19]
SPCE/ZnONR/PMBDES/AuNP	DPV	0.8976	0.1 – 25.0	0.00191	[55]
P-WO ₃ NS/GCE	LSV	0.2	0.01 – 100	0.06	[21]
CS/GCE	DPV	0.02144	40 – 750	0.7	[56]
DDF-CNT-TiO ₂ /IL/GC	DPV	0.039	1.0 – 650.0	0.154	[57]
Pt/MWCNT/PPy/AgNPs	DPV	0.43	0.50 – 5.0	0.15	[58]
MWCNT/Nafion/MAO-A	DPV	0.008 nA $\text{ng mL}^{-1} \text{cm}^{-2}$	0.56 – 2.26	0.2	[59]
GCE/MWCNT-NiO	SWV	9.96	5.98 – 62.8	0.118	[60]
DecA:TBAB(5mg)-CNH/GCE	SWV	0.20	0.50 – 32.71	0.09	This work

MWCNT: multiwalled carbon nanotube; BCG: bromocresol green; NDs-AuNPs-Gr-CSN: a film based on incorporation of nanodiamonds, gold nanoparticles, and graphite anchored in casein; MWCNT-PANI: multiwalled carbon nanotube- poly (aniline); CUCCR: C-undecylcalix[4]resorcinarene; AuNPs@PPyNPs: polypyrrole nanoparticles decorated with gold nanoparticles; SPCE/ZnONR/PMBDES/AuNP: zinc oxide nanorod/polymethylene blue (deep eutectic solvent)/gold nanoparticles modified screen-printed carbon electrode; P-WO₃ NS: phosphorous-doped tungsten trioxide nanosheet; CS: Carbon Spheres; DDF-CNT-TiO₂/IL/GC: functionalized carbon nanotubes with titanium dioxide and benzofuran derivative/ionic liquid modified glassy carbon electrode; Pt/MWCNT/PPy/AgNPs: platinum electrode modified with carbon nanotubes/polypyrrole/silver nanoparticles nanohybrid; MWCNT/Nafion/MAO-A: enzyme monoamine oxidase-A (MAO-A) immobilized by covalent binding on multiwalled carbon nanotubes (MWCNT); GCE/MWCNT-NiO: glassy carbon electrodes modified with multiwalled-carbon-nanotube (MWCNT) doped with nickel oxide nanoparticles;

for serotonin detection.

Finally, the reproducibility of the serotonin voltammetric signals and the interference study in the presence of other compounds of interest using the proposed modified electrode were studied. The inter-day and intra-day repeatability studies were performed to evaluate the sensor precision. In the intra-day repeatability, the 5-HT voltammetric response was measured five times in one day ($n = 5$ for each 5-HT concentration). For the inter-day repeatability, SWV measurements were conducted for three days. Fig. S5a shows the square-wave voltammograms obtained for the detection of three different concentrations of 5-HT using one electrode. The relative standard deviation (RSD) values obtained were 2.60 % for 10 $\mu\text{mol L}^{-1}$, 4.10 % for 20 $\mu\text{mol L}^{-1}$, and 3.52 % for 30 $\mu\text{mol L}^{-1}$ of 5-HT. Fig. S5b summarizes the excellent inter-day reproducibility obtained for detecting three different concentrations of 5-HT with three different electrodes showing RSD results between 1 and 5 %. In addition, the stability of the 5-HT voltammetric

interference of common substances found in biological fluids. The study involved fixing the concentration of 5-HT at 5.0 $\mu\text{mol L}^{-1}$ and adding interfering substances at two different concentration ratios: 1:1 and 10:1

([interferent]: [5-HT]). The potential interferents evaluated included urea, glucose, ascorbic acid, dopamine, caffeine, as well as chloride, sodium, potassium, and sulphate ions. The results of the study were analysed by comparing the analytical response of 5-HT in the presence and absence of interference. Figures S7a and b illustrate the comparison of peak current responses of 5-HT in the absence and presence of the potential interfering compounds. The results indicated that no interference was observed when the interferents were present in a 1:1 and 10:1 excess. This suggests that the proposed electrode demonstrated good selectivity over the set of tested species.

3.8. Analysis of serotonin in synthetic biologic fluids

The DecA:TBAB(5mg)-CNH/GCE electrode was used to detect 5-HT in synthetic urine and bovine serum to assess its suitability for biological fluid analysis. For the analysis, the samples were spiked with three different concentrations of 5-HT and then analysed using SWV under optimized conditions. The recovery values obtained from this analysis, as shown in Table 3, ranged from 92.0 to 101 %. These results indicate that the proposed method to modify GCE with carbon nanohorns composites in HDES has great potential for successfully detecting serotonin in biological samples.

response was assessed using cyclic voltammetry, Figure S6. Even after 100 consecutive cycles, the sensor maintained a stable performance, exhibiting a signal reduction of less than 9 % in the 5-HT oxidation process. This can be attributed to the excellent homogeneity obtained by adding HDES in the film suspension to modify the GCE.

The electrode DecA:TBAB(5mg)-CNH/GCE was used to assess the

4. Conclusions

This study presented a green and cost-effective strategy to enhance the performance of glassy carbon electrodes for serotonin detection by incorporating the DecA:TBAB hydrophobic deep eutectic solvent. Differential scanning calorimetry analysis confirmed the HDES's low melting temperature (lower than 273.15 K), demonstrating its suitability for applications at room temperature. Optimization experiments presented 5 mg of HDES as the ideal amount, achieving improved conductivity, reduced charge transfer resistance, enhanced catalytic efficiency, and increased electroactive surface area.

The simplicity of the HDES-based modification process highlights its potential for further application in the electrochemical detection of other analytes with high sensitivity and precision. Additionally, the environmentally friendly nature of HDES, supported by the EcoScale score and E-factor, aligns with sustainable practices in sensor fabrication.

Despite its promising performance, the approach has a restriction. The viscosity of HDES impacts film conductivity, and higher amounts of HDES negatively affect the analytical signal, emphasizing the importance of optimizing the HDES content. Future research should focus on exploring compatibility with diverse analytes and addressing challenges associated with HDES viscosity to unlock its full potential in sustainable sensor technologies.

Table 3
Determination of serotonin in spiked synthetic urine and bovine serum using the proposed electrode DecA:TBAB(5mg)-CNH/GCE.

Sample ^a	[5-HT]		
	Added / μM	Found / μM	Recovery ^b / %
Synthetic urine	2.0	1.98 \pm 0.09	99.0
	3.0	2.79 \pm 0.09	93.0
	5.0	5.07 \pm 0.03	101
Bovine serum	2.0	1.84 \pm 0.03	92.0
	3.0	2.87 \pm 0.09	95.7
	5.0	4.9 \pm 0.2	98.2

^a $n=3$;

^b Recovery = $([\text{5-HT}]_{\text{Found}}/[\text{5-HT}]_{\text{Added}}) \times 100$ %.

Declaration of competing interest

The authors declare that they have no known competing financial interests or personal relationships that could have appeared to influence the work reported in this paper.

Acknowledgements

The authors thank Conselho Nacional de Desenvolvimento Científico e Tecnológico – CNPq (grant numbers 140406/2021–2 and 401681/2023–8), Fundação Coordenação de Aperfeiçoamento de Pessoal de Nível Superior – CAPES (finance code 001 and CAPES-Print 88887.836030/2023–00), National Institute of Science and Technology of Nanomaterials for Life (INCT NanoVida) (CNPq grant 406079/2022–6), Fundação de Amparo à Pesquisa do Estado de São Paulo – FAPESP (grant numbers 2024/04116–8 and 2024/13620-1) and Horizon Europe grant 101137990 for the financial support granted during this research and thank the Laboratory of Structural Characterization (LCE/DEMa/UFSCar) for the general facilities.

Supplementary materials

Supplementary material associated with this article can be found, in the online version, at [doi:10.1016/j.electacta.2025.145836](https://doi.org/10.1016/j.electacta.2025.145836).

Data availability

Data will be made available on request.

References

- [1] E.L. Smith, A.P. Abbott, K.S. Ryder, Deep eutectic solvents (DESs) and their applications, *Chem. Rev.* 114 (2014) 11060–11082, <https://doi.org/10.1021/CR300162P>.
- [2] A.P.R. Santana, J.A. Mora-Vargas, T.G.S. Guimarães, C.D.B. Amaral, A. Oliveira, M. H. Gonzalez, Sustainable synthesis of natural deep eutectic solvents (NADES) by different methods, *J. Mol. Liq.* 293 (2019) 111452, <https://doi.org/10.1016/j.molliq.2019.111452>.
- [3] M. Simone, M. Pulpito, F.M. Perna, V. Capriati, P. Vitale, Switchable deep eutectic solvents for sustainable sulfonamide synthesis, *Chemistry – A European Journal* (2024), <https://doi.org/10.1002/chem.202402293>.
- [4] A.P. Abbott, Deep eutectic solvents and their application in electrochemistry, *Curr. Opin. Green. Sustain. Chem.* 36 (2022) 100649, <https://doi.org/10.1016/j.cogsc.2022.100649>.
- [5] C.M.A. Brett, Deep eutectic solvents and applications in electrochemical sensing, *Curr. Opin. Electrochem.* 10 (2018) 143–148, <https://doi.org/10.1016/j.coelec.2018.05.016>.
- [6] A.P. Abbott, A. Ballantyne, R.C. Harris, J.A. Juma, K.S. Ryder, A comparative study of nickel electrodeposition using deep eutectic solvents and aqueous solutions, *Electrochim. Acta* 176 (2015) 718–726, <https://doi.org/10.1016/j.electacta.2015.07.051>.
- [7] W. da Silva, A.C. Queiroz, C.M.A. Brett, Nanostructured poly(Phenazine)/Fe2O3 nanoparticle film modified electrodes formed by electropolymerization in ethaline – deep eutectic solvent. Microscopic and electrochemical characterization, *Electrochim. Acta* 347 (2020) 136284, <https://doi.org/10.1016/j.electacta.2020.136284>.
- [8] J.M.S. Almeida, Z.S.B. Pedro, R.M. Buoro, C.M.A. Brett, Binary and ternary deep eutectic solvents for methylene green electropolymerization on multiwalled carbon nanotubes: optimization, characterization and application, *Chemistry – A European J.* (2024) e202401752, <https://doi.org/10.1002/CHEM.202401752>.
- [9] P.C. Gomes-Junior, K.K. de Lima Augusto, G.P. Longatto, R. de Oliveira Gonçalves, T.A. Silva, E. T.G. Cavalheiro, O. Fatibello-Filho, Ultrasmall platinum nanoparticles synthesized in reline deep eutectic solvent explored towards the voltammetric sensing of riboflavin in beverages and biological fluids, *Sens. Actuators. B Chem.* 395 (2023) 134489, <https://doi.org/10.1016/j.snb.2023.134489>.
- [10] P.C. Gomes-Junior, G.P. Longatto, K.K. de Lima Augusto, J. da Silveira Rocha, E. Piccin, O. Fatibello-Filho, Synthesis of ultrasmall cerium oxide nanoparticles in deep eutectic solvent and their application in an electrochemical sensor to detect dopamine in biological fluid, *Microchimica Acta* 191 (2024) 1–12, <https://doi.org/10.1007/S00604-024-06480-4/METRICS>.
- [11] R.M. Buoro, J.M.S. Almeida, C.M.A. Brett, Cresyl violet electropolymerization on functionalized multiwalled carbon nanotubes in carboxylic acid based ternary deep eutectic solvents for hydroquinone sensing, *Electrochim. Acta* 490 (2024) 144305, <https://doi.org/10.1016/j.electacta.2024.144305>.
- [12] K.P. Prathish, R.C. Carvalho, C.M.A. Brett, Electrochemical characterisation of poly(3,4-ethylenedioxythiophene) film modified glassy carbon electrodes prepared in deep eutectic solvents for simultaneous sensing of biomarkers, *Electrochim. Acta* 187 (2016) 704–713, <https://doi.org/10.1016/j.electacta.2015.11.092>.
- [13] A. Ahmadi, S.M. Khoshfetrat, Z. Mirzaeizadeh, S. Kabiri, J. Rezaie, K. Omidfar, Electrochemical immunosensor for determination of cardiac troponin I using two-dimensional metal-organic framework/Fe3O4–COOH nanosheet composites loaded with thionine and pCTAB/DES modified electrode, *Talanta* 237 (2022) 122911, <https://doi.org/10.1016/j.talanta.2021.122911>.
- [14] I. Uysal, B. Dalkiran, O. Atakol, Electrosynthesis of toluidine blue on Fe3O4 nanoparticles modified electrodes in a deep eutectic solvent for the electrochemical determination of neurotransmitter epinephrine, *Microchemical J.* 199 (2024) 109986, <https://doi.org/10.1016/j.microc.2024.109986>.
- [15] W. da Silva, C.M.A. Brett, Novel biosensor for acetylcholine based on acetylcholinesterase/poly(neutral red) – Deep eutectic solvent/Fe2O3 nanoparticle modified electrode, *J. Electroanal. Chem.* 872 (2020) 114050, <https://doi.org/10.1016/j.jelechem.2020.114050>.
- [16] S. Sharma, N. Singh, V. Tomar, R. Chandra, A review on electrochemical detection of serotonin based on surface modified electrodes, *Biosens. Bioelectron.* 107 (2018) 76–93, <https://doi.org/10.1016/j.bios.2018.02.013>.
- [17] K. Khoshevisan, E. Honarvarfard, F. Torabi, H. Maleki, H. Baharifar, F. Faridbod, B. Larjani, M.R. Khorramizadeh, Electrochemical detection of serotonin: a new approach, *Clinica Chimica Acta* 501 (2020) 112–119, <https://doi.org/10.1016/j.cca.2019.10.028>.
- [18] B. Uslu, S.A. Ozkan, Electroanalytical methods for the determination of pharmaceuticals: a review of recent trends and developments, *Anal Lett* 44 (2011) 2644–2702, <https://doi.org/10.1080/00032719.2011.553010>.
- [19] M. Tertiş, A. Cernat, D. Lacaţiş, A. Florea, D. Bogdan, M. Suci, R. Şandulescu, C. Cristea, Highly selective electrochemical detection of serotonin on polypyrrole and gold nanoparticles-based 3D architecture, *Electrochem. commun.* 75 (2017) 43–47, <https://doi.org/10.1016/j.jelechem.2016.12.015>.
- [20] G. Ran, Y. Xia, L. Liang, C. Fu, Enhanced response of sensor on serotonin using nickel-reduced graphene oxide by atomic layer deposition, *Bioelectrochemistry.* 140 (2021) 107820, <https://doi.org/10.1016/j.bioelechem.2021.107820>.
- [21] S. Musuvadhi Babulal, H.F. Wu, C. Chien Wu, Two-dimensional phosphorus-doped tungsten trioxide nanosheets for electrochemical detection of serotonin in biological fluids, *ACS. Appl. Nano Mater.* 6 (2023) 14552–14562, <https://doi.org/10.1021/ACSANM.3C02724>.
- [22] E. Koluçak, S. U. Karabiberoglu, Z. Dursun, Electrochemical determination of serotonin using pre-treated multi-walled carbon nanotube-polyaniline composite electrode, *Electroanalysis.* 30 (2018) 2977–2987, <https://doi.org/10.1002/ELAN.201800588>.
- [23] G. Ran, X. Chen, Y. Xia, Electrochemical detection of serotonin based on a poly (bromocresol green) film and Fe3O4 nanoparticles in a chitosan matrix, *RSC. Adv.* 7 (2017) 1847–1851, <https://doi.org/10.1039/C6RA25639B>.
- [24] K.K. de L. Augusto, G.R. Piton, P.C. Gomes-Junior, G.P. Longatto, F.C. de Moraes, O. Fatibello-Filho, Enhancing the electrochemical sensitivity of hydroquinone using a hydrophobic deep eutectic solvent-based carbon paste electrode, *Analytical Methods* 14 (2022) 2003–2013.
- [25] L.S.S. Cariati, R.M. Buoro, Evaluation of ionic natural deep eutectic solvents (NADES) modified binders towards the chemical properties of carbon paste electrodes, *Electrochem. commun.* 109 (2019) 106605, <https://doi.org/10.1016/j.elechem.2019.106605>.
- [26] G.R. Piton, K.K.L. Augusto, A. Wong, F.C. Moraes, O. Fatibello-Filho, A novel electrochemical glassy carbon electrode modified with carbon black and glycine deep eutectic solvent within a crosslinked chitosan film for simultaneous determination of acetaminophen and diclofenac, *Electroanalysis.* 33 (2021) 1–11, <https://doi.org/10.1002/ELAN.202100325>.
- [27] R. Bavandpour, M. Rajabi, H. Karimi-Maleh, A. Asghari, Application of deep eutectic solvent and SWCNT-ZrO2 nanocomposite as conductive mediators for the fabrication of simple and rapid electrochemical sensor for determination of trace anti-migration drugs, *Microchemical J.* 165 (2021) 106141, <https://doi.org/10.1016/j.microc.2021.106141>.
- [28] T. Atici, M. Bilgi Kamaç, M. Yılmaz, A. Yılmaz Kabaca, Zinc oxide nanorod/polymethylene blue (deep eutectic solvent)/gold nanoparticles modified electrode for electrochemical determination of serotonin (5-HT), *Electrochim. Acta* 458 (2023) 142484, <https://doi.org/10.1016/j.electacta.2023.142484>.
- [29] A. Yılmaz Kabaca, M. Bilgi Kamaç, M. Yılmaz, T. Atici, Ultra-sensitive electrochemical sensors for simultaneous determination of dopamine and serotonin based on titanium oxide-gold nanoparticles-poly nile blue (in deep eutectic

- solvent), *Electrochim. Acta* 467 (2023) 143046, <https://doi.org/10.1016/j.electacta.2023.143046>.
- [30] N. Laube, B. Mohr, A. Hesse, Laser-probe-based investigation of the evolution of particle size distributions of calcium oxalate particles formed in artificial urines, *J. Cryst. Growth* 233 (2001) 367–374, [https://doi.org/10.1016/S0022-0248\(01\)01547-0](https://doi.org/10.1016/S0022-0248(01)01547-0).
- [31] R.A. Sheldon, The E Factor: fifteen years on, *Green Chem.* 9 (2007) 1273, <https://doi.org/10.1039/b713736m>.
- [32] K. Van Aken, L. Streckowski, L. Patiny, EcoScale, a semi-quantitative tool to select an organic preparation based on economical and ecological parameters, *Beilstein. J. Org. Chem.* 2 (2006), <https://doi.org/10.1186/1860-5397-2-3>.
- [33] Q. Zhang, K. De Oliveira Vigier, S. Royer, F. Je´roˆme, Deep eutectic solvents: syntheses, properties and applications, *Chem. Soc. Rev.* 41 (2012) 7108–7146, <https://doi.org/10.1039/C2CS35178A>.
- [34] I.M. Sutjahja, S. Wonorahardjo, S. Wonorahardjo, Study on physicochemical and thermal properties of tetrabutylammonium-based cation ionic salts induced by Al₂O₃ additive for thermal energy storage application, *Inorganics. (Basel)* 8 (2020) 51, <https://doi.org/10.3390/INORGANICS8090051>, 2020, Vol. 8, Page 51.
- [35] A. Alhadid, L. Mokrushina, M. Minceva, Design of deep eutectic systems: a simple approach for preselecting eutectic mixture constituents, *Molecules.* 25 (2020) 1077, <https://doi.org/10.3390/MOLECULES25051077>, 2020, Vol. 25, Page 1077.
- [36] G.J. Maximo, N.D.D. Carareto, M.C. Costa, A.O. dos Santos, L.P. Cardoso, M. A. Kr´ahenbühl, A.J.A. Meirelles, On the solid–liquid equilibrium of binary mixtures of fatty alcohols and fatty acids, *Fluid. Phase Equilib.* 366 (2014) 88–98, <https://doi.org/10.1016/J.FLUID.2014.01.004>.
- [37] T. Pajkossy, Impedance spectroscopy at interfaces of metals and aqueous solutions — Surface roughness, CPE and related issues, *Solid. State Ion.* 176 (2005) 1997–2003, <https://doi.org/10.1016/J.SSI.2004.06.023>.
- [38] N.O. Laschuk, E.B. Easton, O.V. Zenkina, Reducing the resistance for the use of electrochemical impedance spectroscopy analysis in materials chemistry, *RSC. Adv.* 11 (2021) 27925–27936, <https://doi.org/10.1039/D1RA03785D>.
- [39] S. Ruggeri, F. Poletti, C. Zanardi, L. Pigani, B. Zanfognini, E. Corsi, N. Dossi, M. Salom´aki, H. Kivel´a, J. Lukkari, F. Terzi, Chemical and electrochemical properties of a hydrophobic deep eutectic solvent, *Electrochim. Acta* 295 (2019) 124–129, <https://doi.org/10.1016/J.ELECTACTA.2018.10.086>.
- [40] L. Guan, L. Yu, G.Z. Chen, Capacitive and non-capacitive faradaic charge storage, *Electrochim. Acta* 206 (2016) 464–478, <https://doi.org/10.1016/j.electacta.2016.01.213>.
- [41] Zbigniew Galus, *Fundamentals of Electrochemical Analysis*, Ellis Horwood, Chichester, New York, 1976.
- [42] P. Cardoso Gomes-Junior, E. Dias Nascimento, K. Kenlender de Lima Augusto, G. Patelli Longatto, R. Censi Faria, E. Piccin, O. Fatibello-Filho, Voltammetric determination of uric acid using a miniaturized platform based on screen-printed electrodes modified with platinum nanoparticles, *Microchemical J.* 207 (2024) 111931, <https://doi.org/10.1016/j.microc.2024.111931>.
- [43] F. Wang, Y. Wu, K. Lu, B. Ye, A simple but highly sensitive and selective calixarene-based voltammetric sensor for serotonin, *Electrochim. Acta* 87 (2013) 756–762, <https://doi.org/10.1016/J.ELECTACTA.2012.09.033>.
- [44] H. Filik, A.A. Avan, S. Aydar, Square-wave adsorptive stripping voltammetric determination of serotonin at glassy carbon electrode modified with safranine O, *Int. J. Electrochem. Sci.* 9 (2014) 2922–2933, [https://doi.org/10.1016/S1452-3981\(23\)07979-8](https://doi.org/10.1016/S1452-3981(23)07979-8).
- [45] T. Azami, D. Kasuya, R. Yuge, M. Yudasaka, S. Iijima, T. Yoshitake, Y. Kubo, Large-scale production of single-wall carbon nanohorns with high purity, *Journal of Physical Chemistry C* 112 (2008) 1330–1334, <https://doi.org/10.1021/JP076365O>.
- [46] Z. Galus, *Fundamentals of Electrochemical Analysis*, Ellis Horwood, New York, 1976.
- [47] N.K. Sadanandhan, M. Cheriyaathuchenaaramvalli, S.J. Devaki, A.R. Ravindranatha Menon, PEDOT-reduced graphene oxide-silver hybrid nanocomposite modified transducer for the detection of serotonin, *J. Electroanalytical Chem.* 794 (2017) 244–253, <https://doi.org/10.1016/J.JELECHEM.2017.04.027>.
- [48] M.G. Trachioti, A.Ch. Lazanas, M.I. Prodromidis, Shedding light on the calculation of electrode electroactive area and heterogeneous electron transfer rate constants at graphite screen-printed electrodes, *Microchimica Acta* 190 (2023) 251, <https://doi.org/10.1007/s00604-023-05832-w>.
- [49] V. Kathiresan, T. Rajarathinam, S. Lee, S. Kim, J. Lee, D. Thirumalai, S.-C. Chang, Cost-effective electrochemical activation of graphitic carbon nitride on the glassy carbon electrode surface for selective determination of serotonin, *Sensors* 20 (2020) 6083, <https://doi.org/10.3390/s20216083>.
- [50] X. Jiang, X. Lin, Overoxidized polypyrrole film directed DNA immobilization for construction of electrochemical micro-biosensors and simultaneous determination of serotonin and dopamine, *Anal. Chim. Acta* 537 (2005) 145–151, <https://doi.org/10.1016/J.ACA.2005.01.049>.
- [51] A. Bard, L. Faulkner, *Electrochemical Methods: Fundamentals and Applications*, Wiley, New York, 2001.
- [52] G. Ran, Y. Li, Y. Xia, Graphene oxide and electropolymerized p-aminobenzenesulfonic acid mixed film used as dopamine and serotonin electrochemical sensor, *Monatsh. Chem.* 151 (2020) 293–299, <https://doi.org/10.1007/S00706-020-02559-9/METRCS>.
- [53] G. Ran, X. Chen, Y. Xia, Electrochemical detection of serotonin based on a poly (bromocresol green) film and Fe 3 O 4 nanoparticles in a chitosan matrix, *RSC. Adv.* 7 (2017) 1847–1851, <https://doi.org/10.1039/C6RA25639B>.
- [54] M.M.V. Ramos, J.H.S. Carvalho, P.R. de Oliveira, B.C. Janegitz, Determination of serotonin by using a thin film containing graphite, nanodiamonds and gold nanoparticles anchored in casein, *Measurement* 149 (2020) 106979, <https://doi.org/10.1016/J.MEASUREMENT.2019.106979>.
- [55] T. Atici, M. Bilgi Kamaç, M. Yılmaz, A. Yılmaz Kabaca, Zinc oxide nanorod/ polymethylene blue (deep eutectic solvent)/gold nanoparticles modified electrode for electrochemical determination of serotonin (5-HT), *Electrochim. Acta* 458 (2023) 142484, <https://doi.org/10.1016/J.ELECTACTA.2023.142484>.
- [56] J. Zhou, M. Sheng, X. Jiang, G. Wu, F. Gao, Simultaneous determination of dopamine, serotonin and ascorbic acid at a glassy carbon electrode modified with carbon-spheres, *Sensors* 13 (2013) 14029–14040, <https://doi.org/10.3390/s131014029>.
- [57] M. Mazloum-Ardakani, A. Khoshroo, Electrocatalytic properties of functionalized carbon nanotubes with titanium dioxide and benzofuran derivative/ionic liquid for simultaneous determination of isoproterenol and serotonin, *Electrochim. Acta* 130 (2014) 634–641, <https://doi.org/10.1016/j.electacta.2014.03.063>.
- [58] I. Cesarino, H.V. Galesco, S.A.S. Machado, Determination of serotonin on platinum electrode modified with carbon nanotubes/polypyrrole/silver nanoparticles nanohybrid, *Materials Sci. Eng C* 40 (2014) 49–54, <https://doi.org/10.1016/j.msec.2014.03.030>.
- [59] A. Becerra-Herna´ndez, J. Galindo-de-la-Rosa, Y. Martınez-Pimentel, J. Ledesma-Garcıa, L. A´lvarez-Contreras, M. Guerra-Balca´zar, A. Aguilar-Elguezabal, A. A´lvarez, A.U. Cha´vez-Ramırez, V. Vallejo-Becerra, Novel biomaterial based on monoamine oxidase-A and multi-walled carbon nanotubes for serotonin detection, *Biochem. Eng. J.* 149 (2019) 107240, <https://doi.org/10.1016/j.bej.2019.107240>.
- [60] O.E. Fayemi, A.S. Adekunle, E.E. Ebenso, Electrochemical determination of serotonin in urine samples based on metal oxide nanoparticles/MWCNT on modified glassy carbon electrode, *Sens. Biosensing. Res.* 13 (2017) 17–27, <https://doi.org/10.1016/j.sbsr.2017.01.005>.